


Optical detection of the periodic variability at the white dwarf GD 394 with TESS

DAVID J. WILSON ¹, BORIS T. GÄNSICKE,² AND J. J. HERMES³

¹*McDonald Observatory, University of Texas at Austin, Austin, TX 78712*

²*Department of Physics, University of Warwick, Coventry CV4 7AL, UK*

³*Department of Astronomy, Boston University, 725 Commonwealth Ave., Boston, MA 02215, USA*

(Received January 27, 2020; Revised January 27, 2020; Accepted January 27, 2020)

Submitted to ApJL

ABSTRACT

We present observations obtained with the *Transiting Exoplanet Survey Satellite* (*TESS*) of the white dwarf GD 394. The space-based optical photometry demonstrates a 0.12 ± 0.01 per cent flux variation with a period of 1.146 ± 0.001 d, consistent with the 1.150 ± 0.003 d period variation detected in observations obtained with the *Extreme Ultraviolet Explorer* in the mid 1990s. We describe the analysis of the *TESS* light curve and measurement of the optical variation, and discuss the implications of our results for the various physical explanations put forward for the variability of GD 394.

1. INTRODUCTION

GD 394 is a hot, metal-polluted white dwarf that has presented challenges to astronomers since its initial identification by Giclas et al. (1967). Indeed, both of the descriptions in the preceding sentence are unquantified: Estimates for the effective temperature vary from 33000–41000 K (Lajoie & Bergeron 2007; Barstow et al. 1996) and the measured metal abundances, accretion rates and species depends on the wavelength band and ionisation levels observed (Wilson et al. 2019). However, the most intriguing aspect of GD 394 is the detection by Christian et al. (1999) and Dupuis et al. (2000) of a sustained 25 per cent modulation of the extreme ultraviolet (EUV) flux with a period of 1.15 d, identified in observations made in 1992–1996 with multiple instruments onboard the *Extreme Ultraviolet Explorer* (*EUVE*) satellite. This phenomenon is thus far unique among white dwarfs, and was hypothesised to be due to opacity changes induced by a spot of accreting metals rotating in to and out of view with the white dwarf rotation.

The spot hypothesis made two observable predictions: Firstly, the strength of the metal lines in the white dwarf spectrum should vary in phase with the EUV variation; secondly, there should be an anti-phase flux variation at optical wavelengths due to flux redistribution. Follow-up observations by Wilson et al. (2019) ruled out the first of these predictions, finding no change in the strength of the metal lines in eight *Hubble Space Telescope* (*HST*) far ultraviolet (FUV) spectra sampling the full (putative) white dwarf spin cycle. They also searched SuperWASP photometry for optical variation, ruling out changes in flux \gtrsim one per cent. Instead of a spot model, Wilson et al. (2019) favoured a circumstellar explanation such as a gas cloud generated by an evaporating but non-transiting planet, similar to the ice giant detected in orbit of WD J0914+1914 by Gänsicke et al. (2019). Veras & Wolszczan (2019) suggested instead that an orbiting, iron rich planetesimal core could induce a magnetic flux tube connecting it to the white dwarf, heating the photosphere at the base of the tube to produce a hot spot.

Here, we present observations of GD 394 obtained using the *Transiting Exoplanet Survey Satellite* (*TESS*, Ricker et al. 2014) demonstrating that GD 394 is indeed varying in the optical with a period consistent with that of the EUV variation, but with an amplitude much smaller than in the EUV and below the SuperWASP detection limits.

2. OBSERVATIONS

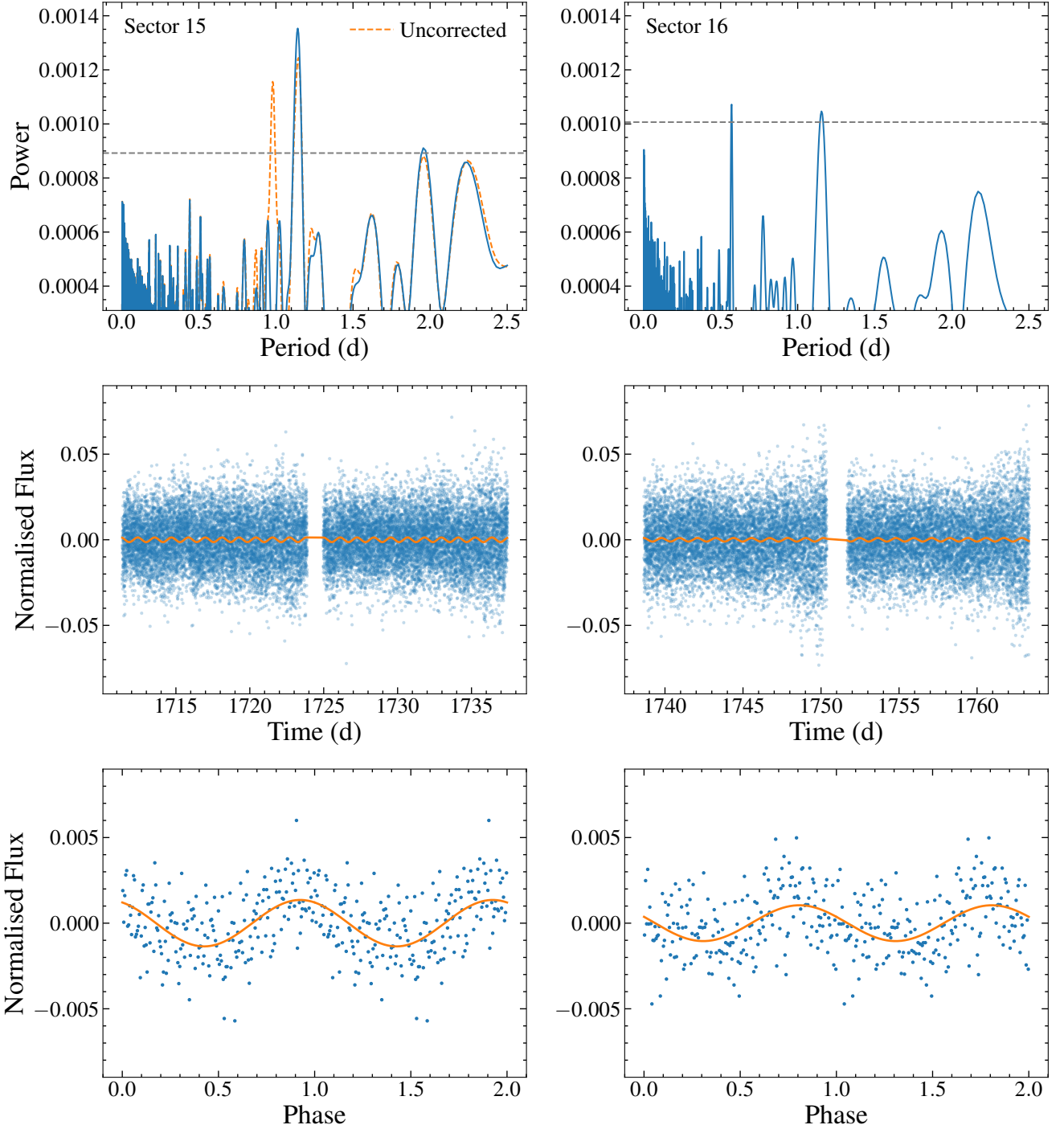


Figure 1. Top: Periodograms of the *TESS* light curves of GD 394 from Sectors 15 and 16. Strong signals at ≈ 1.15 d are detected in each Sector. The grey dashed line shows the 99 percent false alarm probability for each Sector. The orange dashed line shows the periodogram for Sector 15 before removal of the ≈ 0.98 d signal from a nearby star. The first harmonic ($P/2$) of the 1.15 d signal is detected in Sector 16. Middle: *TESS* light curves of GD 394 together with the sine fit used to measure the period and amplitude of the variation. The enhanced scatter at the end of each segment of the light curve is due to increased background Earthshine as the spacecraft approaches perigee. Bottom: Light curves folded onto the fitted period and binned to 3 hours. The cycle is repeated for clarity, and the model fit is overplotted in orange.

Sector	Period (d)	Amplitude (%)
15	1.142 ± 0.003	0.25 ± 0.03
16	1.155 ± 0.005	0.17 ± 0.03
Average	1.145 ± 0.006	0.21 ± 0.04

Table 1. Measured periods and amplitudes for the variation at GD 394.

GD 394 was observed by *TESS* in Camera 2 for 52 days in Sectors 15 and 16 (2019 August 15–2019-October-06), with three roughly one-day gaps at spacecraft perigee¹. Data was returned with a two minute cadence as requested in proposals G022077, G022028 and G022017, and processed using the Pre-Search Data Conditioning Pipeline (PDC, [Stumpe et al. 2012](#)) to remove common known instrumental trends.

We analysed the light curves from each Sector separately. The light curves were retrieved from MAST² and points marked with a quality flag were removed, as were any 5-sigma outliers. The flux was normalised by subtracting a two-order polynomial fit. We generated Lomb-Scargle periodograms using the *Lightkurve* package ([Lightkurve Collaboration, 2018](#)) (Figure 1, top). A ≈ 1.15 d period is clearly detected in each Sector, providing the first confirmation of the *EUVE* detection beyond the extreme ultraviolet.

The Sector 15 periodogram contained a second peak at ≈ 0.98 d (orange dashed line in Figure 1). Using the *TESS* pixel data, we found that this signal originates from a nearby giant star, Gaia 2166114911196097024 ([Gaia Collaboration et al. 2018](#)). We divided out a sinusoidal fit to the data at the spurious period, and recomputed the periodogram to confirm that the signal was successfully removed.

To ascertain the significance of the detected signals we calculated the false alarm probability (FAP) via the method used in [Hermes et al. \(2017\)](#); [Bell et al. \(2019\)](#). We generated 10000 fake light curves for each Sector, using the same time-axis but randomly shuffling the flux values. A periodogram was calculated for each fake light curve and the maximum power recorded. We defined our one per cent FAP as the power below which the maximum power in 99 per cent of our fake light curves fell (grey dashed line in Figure 1). As the signals in each light curve exceed this limit, we conclude that there is a less than one per cent probability that our detected signal is due to random chance.

We then fit a sinusoidal curve to each light curve using the peak measured from the periodogram as an initial guess. The middle panel of Figure 1 shows the fits to the light curves, and the bottom panel shows the data folded onto the fitted period. The measured amplitudes were then divided by the "CROWDSAP" value in the fits headers (0.55265564 and 0.59237289 for Sectors 15 and 16 respectively) to account for crowding by nearby sources in the aperture. Our results are presented in Table 1.

Whilst the periods and amplitudes for each Sector are different, they are within 3sigma of each other so we do not claim a detection of variation between the two Sectors, and take the average values of the two Sectors as our final result. The measured amplitude should only be taken as an approximate value as the true variation may have a more complex behaviour than a simple sine wave, such as the spot model fit to the *EUVE* data by [Dupuis et al. \(2000\)](#).

3. DISCUSSION AND CONCLUSION

The $P = 1.145 \pm 0.006$ d period variation of GD 394 in the *TESS* light curve is consistent with the 1.150 ± 0.003 d period measured in the *EUVE* data by [Dupuis et al. \(2000\)](#). The variation in the two wavebands therefore almost certainly have the same origin, and there is no strong evidence for period evolution in the roughly 24 years between the observations. On the other hand, the optical amplitude of 0.21 ± 0.04 per cent is much smaller than the ≈ 25 per cent variation in the EUV.

The *TESS* observations support the prediction made by [Dupuis et al. \(2000\)](#) that, if the EUV variation is due to opacity changes caused by a spot of metals, an anti-phase variation in the optical would be produced by flux redistribution. However, the metal spot model was ruled out by the non-detection of changes in the metal absorption line strengths by [Wilson et al. \(2019\)](#). It is possible that the spot has a variable opacity, appearing strongly at the time of the *EUVE* observations, fading by the time of the 2015 *HST* observations but returning in time to be observed with *TESS* (with the period fixed by the white dwarf rotation period) but this may be too strong an appeal to coincidence, especially considering that the 2015 *HST* spectra were consistent with *HST* spectra obtained in 1992 by [Shipman et al. \(1995\)](#).

¹ See *TESS* Data Release Notes at http://archive.stsci.edu/tess/tess_drn.html

² <https://archive.stsci.edu/>

We are left requiring a mechanism that will generate flux variations of 25 per cent in the EUV, 0.21 per cent in the optical, and $\lesssim 1$ per cent in the FUV (the upper limit placed by light curves extracted from the time-tagged *HST* spectroscopy by Wilson et al. (2019)). The suggestion by Veras & Wolszczan (2019) that the variation is due to a hot spot at the base of a magnetic flux tube may fit these criteria, as a sufficiently hot spot could provide the required amplitude in the EUV, with the flux quickly dropping away in the Rayleigh–Jeans tail to the low levels observed at longer wavelengths. However, this would require spot temperatures of $\gtrsim 10^5$ K, and thus far no magnetic field has been detected in high-resolution spectroscopy of GD 394 ($B_e \leq 12$ kG, Dupuis et al. 2000; Wilson et al. 2019). The generation of a flux tube requires an orbiting metal-rich planetary fragment which may be radio-loud, and thus radio observations might provide an opportunity to test this model (Veras & Wolszczan 2019).

The various explanations for the flux variations at GD 394 could be tested by searching for phase differences between the two wavebands: Out of phase variation would favour a spot; in phase variation would point to a circumstellar cause. In practice, phasing up the *EUVE* and *TESS* observations is impractical given the decades-long gap between them, so new, simultaneous EUV and high-precision optical observations are required, although this will be challenging given current observing facilities.

In conclusion, the *TESS* observations of GD 394 reveal the same 1.15 d periodicity at optical wavelengths that was initially identified in the EUV over two decades ago. The very small amplitude of the optical modulation, 0.12 per cent, explains why this signal remained undetected in previous ground-based observations of GD 394. A physical explanation for this activity remains elusive.

ACKNOWLEDGMENTS

We thank A. Vanderburg for useful advice regarding contamination from nearby stars in *TESS*.

Facilities: *TESS*

Software: Astropy (Astropy Collaboration, 2013), Lightkurve (Lightkurve Collaboration, 2018)

REFERENCES

- Astropy Collaboration, Robitaille, T. P., Tollerud, E. J., et al. 2013, *A&A*, 558, A33, doi: [10.1051/0004-6361/201322068](https://doi.org/10.1051/0004-6361/201322068)
- Barstow, M. A., Holberg, J. B., Hubeny, I., et al. 1996, 279, 1120
- Bell, K. J., Córscico, A. H., Bischoff-Kim, A., et al. 2019, arXiv e-prints, arXiv:1910.04180, <https://arxiv.org/abs/1910.04180>
- Christian, D. J., Craig, N., Cahill, W., Roberts, B., & Malina, R. F. 1999, *AJ*, 117, 2466, doi: [10.1086/300847](https://doi.org/10.1086/300847)
- Dupuis, J., Chayer, P., Vennes, S., Christian, D. J., & Kruk, J. W. 2000, 537, 977, doi: [10.1086/309079](https://doi.org/10.1086/309079)
- Gaia Collaboration, Brown, A. G. A., Vallenari, A., et al. 2018, ArXiv e-prints. <https://arxiv.org/abs/1804.09365>
- Gänsicke, B. T., Schreiber, M. R., Toloza, O., et al. 2019, *Nature*, 576, 61, doi: [10.1038/s41586-019-1789-8](https://doi.org/10.1038/s41586-019-1789-8)
- Giclas, H. L., Burnham, R., & Thomas, N. G. 1967, *Lowell Observatory Bulletin*, 7, 49
- Hermes, J. J., Gänsicke, B. T., Kawaler, S. D., et al. 2017, *ApJS*, 232, 23, doi: [10.3847/1538-4365/aa8bb5](https://doi.org/10.3847/1538-4365/aa8bb5)
- Lajoie, C., & Bergeron, P. 2007, 667, 1126, doi: [10.1086/520926](https://doi.org/10.1086/520926)
- Lightkurve Collaboration, Cardoso, J. V. d. M., Hedges, C., et al. 2018, Lightkurve: Kepler and TESS time series analysis in Python, Astrophysics Source Code Library. <http://ascl.net/1812.013>
- Ricker, G. R., Winn, J. N., Vanderspek, R., et al. 2014, in Society of Photo-Optical Instrumentation Engineers (SPIE) Conference Series, Vol. 9143, Proc. SPIE, 914320, doi: [10.1117/12.2063489](https://doi.org/10.1117/12.2063489)
- Shipman, H. L., Provencal, J., Roby, S. W., et al. 1995, 109, 1220
- Stumpe, M. C., Smith, J. C., Van Cleve, J. E., et al. 2012, *PASP*, 124, 985, doi: [10.1086/667698](https://doi.org/10.1086/667698)
- Veras, D., & Wolszczan, A. 2019, *MNRAS*, 488, 153, doi: [10.1093/mnras/stz1721](https://doi.org/10.1093/mnras/stz1721)
- Wilson, D. J., Gänsicke, B. T., Koester, D., et al. 2019, *MNRAS*, 483, 2941, doi: [10.1093/mnras/sty3218](https://doi.org/10.1093/mnras/sty3218)